Received: 12 November 2021 | Revised: 28 January 2022 | Accepted: 2 March 2022

DOI: 10.1111/joa.13654

Journal of Anatomy ANATOMICAL SOCIETY WILEY

REVIEW ARTICLE

The right ventricle under pressure: Anatomy and imaging in sickness and health

Harrison Stubbs[1,2] | Alexander MacLellan[1,2] | Stephanie Lua[1] | Helen Dormand[1] | Colin Church[1,2]

[1]Scottish Pulmonary Vascular Unit, Golden Jubilee National Hospital, Glasgow, Scotland

[2]University of Glasgow, Glasgow, Scotland

Correspondence
Harrison Stubbs, Scottish Pulmonary Vascular Unit, Golden Jubilee National Hospital, Glasgow, Scotland.
Email: harrison.stubbs@ggc.scot.nhs.uk

Abstract

The right ventricle (RV) is an important structure which serves a multitude of vital physiological functions in health. For many years, the left ventricle has dominated the focus of understanding in both biology and pathophysiology and the RV was felt to be more of a passive structure which rarely had an effect on disease states. However, it is increasingly recognised that the RV is essential to the homoeostasis of normal physiology and disturbances in RV structure and function have a substantial effect on patient outcomes. Indeed, the prognosis of diseases of lung diseases affecting the pulmonary vasculature and left heart disease is intimately linked to the function of the right ventricle. This review sets out to describe the developmental and anatomical complexities of the right ventricle while exploring the modern techniques employed to image and understand its function from a clinical perspective.

1 | INTRODUCTION

The right ventricle (RV) is an important structure which serves a multitude of vital physiological functions in health. For many years, the left ventricle has dominated the focus of understanding in both biology and pathophysiology and the RV was felt to be more of a passive structure which rarely had an effect on disease states (Rigolin et al., 1995). However, it is increasingly recognised that the RV is essential to the homoeostasis of normal physiology and disturbances in RV structure and function has a substantial effect on patient outcomes. Indeed, the prognosis of diseases of lung diseases affecting the pulmonary vasculature and left heart disease is intimately linked to the function of the right ventricle (Noordegraaf et al., 2019).

This review aims to build on the current understanding of right ventricular function and anatomy by examining how these are altered in the disease state of pulmonary hypertension. It will describe, using clinical images, the developmental and anatomical complexities of the right ventricle and demonstrate the changes found as a result of elevated pulmonary vascular. Through a detailed description of the normal structure and contrasting this directly with abnormalities seen in pathological states, it is hoped that this evaluation will bring a deeper understanding of the intricacy of the right ventricle. This is a timely review, given the advances in clinical imaging, particularly with cardiac magnetic resonance imaging (CMRI) becoming a powerful and increasingly available technique for the assessment of pulmonary hypertension.

2 | THE HEALTHY RIGHT VENTRICLE

2.1 | Embryology

In order to fully understand the anatomy of the right ventricle, a discussion of the embryological development is necessary. Morphogenesis of the cardiac and pulmonary systems largely occurs between weeks 3 and 8 of gestation (Tan & Lewandowski, 2020). The heart is derived from the anterior lateral plate of the mesoderm which forms two crescent-shaped cardiac plates that coalesce

together to form the tubular heart. Cardiac looping occurs between days 22 and 23, whereby the apical portion moves leftwards and cephalically and the basal portion rightwards and caudally, leading to the formation of the outline of the four cardiac chambers (Moorman et al., 2003; Tan & Lewandowski, 2020). Septation occurs between the 27th and 37th day of gestation via the fusion of endocardial cushions and within the atria, the septum primum and secundum develop, through which the foramen ovale is formed (Anderson et al., 2003; Tan et al., 1998). The interventricular septum (IVS) develops out of muscular and membranous components and further endocardial tissue gives rise to the tricuspid and mitral valves (Moorman et al., 2003). The truncus arteriosus develops into the aorta and pulmonary artery, which form over their respective ventricles guided by the aorticopulmonary septum (Anderson et al., 2003).

The right-sided cardiac chambers are dominant in the foetal circulation, providing oxygenated blood from the umbilical vein to the systemic foetal circulation via the foramen ovale and the ductus arteriosus (Tan & Lewandowski, 2020). At birth, following the first breath, a rapid decrease in pulmonary vascular resistance occurs with a concomitant increase in the systemic resistance. This causes the foramen ovale to close and the ductus arteriosus to constrict, allowing the RV to pump deoxygenated blood into the now lower pressure pulmonary circulation. Over the following months, RV wall thickness decreases, compliance increases and the adult cardiac structure is cemented (Morton & Brodsky, 2016; Tan et al., 1998).

2.2 | Anatomical position of adult heart

The right ventricle is the most anterior cardiac chamber, marking the majority of the anterior and inferior border of the cardiac silhouette. The shape is complex; when viewed anteriorly, it is convex and when seen laterally, it appears triangular (Ho & Nihoyannopoulos, 2006). The RV gives an impression of entwining around the LV, from which it is separated by the IVS on the lateroposterior wall, a concave structure that bulges into the body of the RV (Mahadevan, 2015). The RV surface is anatomically divided; the anterior wall lies retrosternally, separated from the thoracic wall by the pericardium. The lateral surface is confluent with the right atrium, demarcated by the tricuspid valve. The inferior wall sits near horizontally on the central tendon and muscular surface of the diaphragm, marked from the 6th costal cartilage on the right, through the xiphisternal joint, to the 5th intercostal space on the left, as far as the midclavicular line. The posterior wall is comprised of the IVS (Gray's anatomy - the anatomical basis of clinical practice, 2020).

2.3 | Internal structure

The RV is a hollow, muscular chamber with a wall thickness in health of 2–5 mm with a mass of 25 ± 5 g/m^2 (Foale et al., 1986; Rodrigues et al., 2007). It is comprised of deep and superficial muscle layers; subendocardial fibres are predominant and are confluent with the IVS, preferentially traversing the RV from the base to the apex. Subepicardial fibres are less pronounced and run circumferentially, parallel to the atrioventricular groove and continue onto the LV (Kovacs et al., 2019). The RV arterial supply is predominantly from the right coronary artery (RCA) with additional supply from the conus artery supplying the infundibulum (Tomanek & Angelini, 2019). The acute marginal arteries supply the anterior free wall, the posterior descending artery to the posterior 1/3 of the IVS and the septal branches of the left anterior descending artery to the remaining 2/3 of the IVS (Tomanek & Angelini, 2019). The RV internal anatomy is divided into a three-part structure, allowing comparison to the embryological origins (Daniel & Walton, 1975).

2.3.1 | RV inlet

The RV inflow tract projects anteriorly and leftwards from the RA, from which it is divided by the tricuspid valve and its attaching structures. The fibrous skeleton of the heart is a set of collagenous rings which connect the annuli of the four cardiac values and this forms the margins of the tricuspid valve and separates the RA from the RV (Robert et al., 2013).

Three RV papillary muscles originate from the interior ventricular wall, giving rise to true chordae tendineae, which attach to the tricuspid valve leaflets, preventing valvular prolapse into the RA (Dahou et al., 2019). The eponymous valve has three leaflets named for their positions as anterosuperior (usually the most prominent), inferior and septal. The septal valve leaflet remains relatively fixed, while the anterior and posterior leaflets move into the RV during diastole and snap close during RV systole. Tricuspid regurgitation can occur due to papillary muscle dysfunction or chordae rupture, such as following RV wall ischaemia. Additionally, it can be seen in pulmonary hypertension as a functional consequence of abnormal RV pressure overload (Dahou et al., 2019).

2.3.2 | Trabeculated apical myocardium

The RV apex is thinner walled compared to the rest of the ventricle and has ridged intersecting muscular structures known as trabeculae carneae (Ho & Nihoyannopoulos, 2006). These form the septomarginal band, the supraventricular crest and the moderator band (MB) which play a role in RV contraction (Loukas et al., 2010). The MB inserts at the base of the anterior papillary muscle and extends to the infundibulum and supraventricular crest. Initially felt to be a protective mechanism to prevent RV over-dilation, it is now recognised that the MB has a role in cardiac conduction, incorporating a portion of the right branch bundle of His and disruption to these fibres commonly results in a right distal bundle branch block pattern (Almedia et al., 2020; Loukas et al., 2010). Ventricular pacemaker leads are commonly placed into the RV apex and the location and nature of the trabeculations allow for lead fixation (Hayes & Furman, 2004).

2.3.3 | RV outlet

The RV outflow tract (RVOT) is a tubular structure that extends from the supraventricular crest superiorly and posteriorly towards the pulmonary valve (PV) from which the main pulmonary artery.

(MPA) arises. The RVOT is composed of the RV free wall, the IVS and the conus arteriosus or infundibulum, which extends from the ventricle base to the PV, attaching to the valve leaflets (Gray's anatomy - the anatomical basis of clinical practice, 2020).

2.4 | Right ventricular physiology and function

The primary function of the RV is the active transmission of deoxygenated blood from the venous circulation to the pulmonary arterial system. During cardiac systole, muscle contraction begins in the RV apex and ends 20–50 ms later in the conus. Longitudinal contraction accounts for the majority of RV contraction due to the predominance of longitudinal deep fibres (Kovacs et al., 2019; Kukulski et al., 2000), which is likened to a wind bellows effect. Blood is transmitted to the RV outlet where it is transmitted via helical flow to the MPA. The fraction of blood ejected through the pulmonary valve to the pulmonary circulation (right ventricular ejection fraction, RVEF) is expressed as a percentage of the stroke volume from each cardiac cycle divided by the right ventricular end-diastolic volume (RVEDV) and is one of the key determinants of prognosis in diseases such as pulmonary hypertension (Courand et al., 2015; Ghio et al., 2010).

Aside from its mechanism as a pump, the heart has an array of endocrine functions through the release of natriuretic peptides in response to myocardial stretching and inflammation. The measurement of brain natriuretic peptide (BNP) and/or N-terminal prohormone BNP (NT-proBNP) is used to assess for the presence of RV failure and assess response to treatment in pulmonary hypertension (Lewis et al., 2020).

2.5 | Comparison to the LV

The RV is increasingly recognised as having a vital role in the management and prognosis of cardiopulmonary conditions, after historically being somewhat neglected when compared to the LV (Rigolin et al., 1995; Voelkel et al., 2006). The RV is distinct from the LV both in function and structure due to differences in the force required to effectively pump into their circulatory systems. The LV afterload comprises of the systemic circulation with a mean arterial pressure (MAP) of 65–100 mm Hg, in contrast to the pulmonary circulation where mean pulmonary artery pressure (MPAP) is 14 ± 3 mm Hg (Voelkel et al., 2006). The lower force required during systole means, when compared to the LV, the RV has a decreased ventricular wall thickness (4 mm, 1/3 of the LV) (Foale et al., 1986) and an overall smaller size and mass (around 1/3 of the LV) (Rodrigues et al., 2007). Other distinguishing anatomical differences include the presence of the moderator band, coarse trabeculations, two distinct cardiomyocyte layers as opposed to three in the myoarchitecture and an alternatively arranged and more muscular infundibulum. The RV inlet has several differences, denoted by the tri-leaflet configuration of the tricuspid valve (as opposed to the bicuspid mitral valve), the septal position of the leaflet of the tricuspid valve (as opposed to the anterior leaflet of the mitral valve), the presence of septal papillary attachments to the tricuspid leaflets and the presence of >3 papillary muscles (Gray's anatomy - the anatomical basis of clinical practice, 2020; Robert et al., 2013). In contrast to the left ventricle, the right ventricle coronary blood supply is continuous throughout both systole and diastole (Zong et al., 2005).

Despite key differences between both ventricles, the importance of ventricular interdependency is increasingly being recognised (Naeije & Badagliacca, 2017). The ventricles share a common septum and are surrounded by shared epimyocardial fibres and a semi-flexible pericardium and thus, the distention of one ventricle affects the distensibility and filling of the other (Noordegraaf et al., 2019). This can lead to physiological repercussions in disease states such as pulmonary hypertension.

3 | THE RV UNDER PRESSURE

3.1 | Introduction to pulmonary hypertension

One of the principal diseases that affects the right ventricle is pulmonary hypertension. In normal circumstances, the pulmonary circulation is a low-pressure system, with a normal mean pulmonary artery pressure (mPAP), considered to be in the region of 14.0 ± 3.3 mm Hg (Kovacs et al., 2009). As mentioned, the normal anatomy of the RV reflects this, as it only requires sufficient muscularity to overcome these low pulmonary pressures, in contrast to the much higher systolic pressure required by the LV to propel blood into the systemic circulation. A variety of factors can lead to a progressive rise in pulmonary artery (PA) pressure, with the definition of PH is currently accepted as a mPAP of >20 mm Hg when measured by right heart catheterisation at rest (Simonneau et al., 2019). The causes of PH are myriad and beyond the scope of this paper but critically many involve the development of an arteriopathy in the small vessels with vascular remodelling. They include intrinsic disease of the pulmonary arterial vasculature itself as well as PH arising from chronic thromboembolic disease, left-sided cardiac impairment or parenchymal lung diseases. Rising PA pressures generally result in the RV having to perform a task that it has not been designed for, and the majority of symptoms of worsening PH (of any aetiology) result from its cumulative effects on the RV. The common clinical manifestations of PH include shortness of breath (particularly on exertion), chest pain, peripheral oedema and syncope (the latter often being considered a sign of severe or advancing disease). The disease course is generally progressive and in many cases, PH is life shortening, with a common cause of death being eventual failure of the RV (Rubin & Physicians ACoC., 2004).

3.2 | Changes in RV structure and function in PH

The state of pressure overload related to chronically elevated pulmonary artery pressure results in a number of structural changes to the RV. In the early stages, these are appropriately adaptive, meaning that the RV can retain reasonable function. However, with long-standing or progressive PH, there comes a point where the anatomical changes effected in the RV become overtly pathological and ventricular function begins to inexorably decline (Rao et al., 2019). The various anatomical and functional changes which occur will be discussed in turn.

3.2.1 | RV hypertrophy

The adaptability of the RV is considerable and in fact much greater than that of the LV (Lyon et al., 2015). In order to achieve the impetus required to propel blood through the high impedance pulmonary circulation which exists in PH, the RV undergoes a process of myocardial hypertrophy (Sanz et al., 2019). This involves not only the RV wall but also the trabeculations and muscular bands described earlier (Dong et al., 2018). This adaptive process is triggered by the process of mechanotransduction, through which cardiomyocytes sense and adapt to increasing load. Aggregation of myocytes leads to an adaptive increase in RV mass. There are varying reports of the changes in myoarchitecture which occur in this situation; some experimental models have suggested that myocyte aggregation in this context occurs with preserved RV muscle structure, whilst other studies suggest a more circumferential process (Nielsen et al., 2009; Tezuka et al., 1990). As wall thickness increases, this leads to increased wall tension and relative ischaemic areas, which further weakens the RV.

3.2.2 | Abnormalities of the interventricular septum

The systolic motion of the IVS is mediated by a superficial layer of myocardial fibres which are continuous with those of the LV (Ryan & Archer, 2014). The state of pressure overload caused by PH results in abnormal bowing of the IVS into the LV (Bidviene et al., 2021). Early in the process, this can be observed as a septal 'bounce' towards the LV during systole. In more severe states of pressure overload, the septum can become markedly displaced towards the LV for the entirety of the cardiac cycle. As a consequence, the left-sided chambers can become compressed and the LV adopts a smaller, crescentic shape normally associated with the healthy RV.

3.2.3 | Myocardial fibrosis

The adaptive increase in RV mass described earlier brings with it an increased oxygen demand. Relative RV ischaemia can occur due to the inability of the coronary circulation to adequately perfuse additional myocardial tissue. This can be compounded in some cases by compression of the left or RCA by a dilated MPA (van Wolferen et al., 2008), which can result in significant chest pain for patients. Although it is unusual to observe macroscopic areas of infarction in the RV, episodes of ischaemia can, over time, lead to RV myocardial fibrosis (Baggen et al., 2016). The fibrotic change tends to be less marked in patients with congenital heart disease (e.g., Eisenmenger syndrome), suggesting that the long-standing nature of CHD leads to better adaptation (Gomez-Arroyo et al., 2014). Areas of fibrosis can also act as a substrate for the onset of cardiac arrhythmias which can lead to sudden death in these patients.

3.2.4 | RV dilatation and failure

Following the development of concentric RV hypertrophy, continued pressure overload in the ventricle begins to cause a process of more eccentric myocardial hypertrophy. This leads to a less robust myocardial structure which is then prone to progressive dilatation (Vonk-Noordegraaf et al., 2013). Markedly elevated RV afterload eventually exhausts the adaptive abilities of the RV and contractility begins to suffer. At this stage, the nature of RV contraction begins to alter, with less longitudinal contraction and greater reliance on motion of the transverse wall (Kind et al., 2010). A state of dyssynchrony with the LV develops, resulting in mechanical inefficiency and reduction in RV ejection fraction. This reduction in function has a tendency to progress to the stage where the RV can no longer sufficiently augment systemic cardiac output due to a drop in left-sided pre-load. In addition, physical compression of the LV by severely dilated right-sided chambers can directly affect the LV filling capabilities. Both of these mechanisms contribute to worsening clinical manifestations of right ventricular failure.

4 | IMAGING OF THE RV IN PULMONARY HYPERTENSION

In this section, we look at the imaging techniques used to assess RV function and determine the aetiology of the disease. These techniques are used in tandem with pulmonary imaging to provide as accurate an assessment in clinical practice. Traditionally, a conventional transthoracic echocardiogram was the imaging modality of choice for the right ventricle due to ease of access, relative costs and the availability of trained technicians. However, the accuracy of RV assessment is limited by its complex anatomy and retrosternal location. Other factors affecting accuracy include increased adipose tissue and end-stage pulmonary disease, as the acoustic windows required for specific views are often difficult to obtain in these situations. It is intuitively felt that treatment and pulmonary arterial dilation would improve right ventricle function; yet increasingly, this is found to be inaccurate and therefore begs the need to accurately track RV changes and function during the course of disease.

4.1 | Chest X-Ray (CXR)

CXR is often of the first non-invasive investigations performed in a dyspnoeic patient. It is a 2D image that provides useful information on both cardiac and lung pathologies. Whilst relatively cheap and easy to access, CXR has a poor sensitivity and specificity rate for picking up RV pathology; the main function of a CXR is usually to exclude lung pathology leading to dyspnoea such as pneumothorax, pneumonia or rib fractures. Cardiac pathologies on CXR are more subtle and often missed, especially in the early stages of disease. Indeed, a normal chest x-ray does not exclude RV pathology. In early stages of pulmonary hypertension, CXR may be normal, or early subtle changes such as an enlarged pulmonary trunk may be seen. In congenital heart disease, cardiomegaly can often be associated with the appearance of plethoric vessels which can often be mistaken for pulmonary oedema. RV ventricular hypertrophy and dilatation can appear on a CXR as a rounded left heart border with a raised cardiac apex. As disease progresses, RV failure can occur and can result in cardiomegaly (Figure 1).

4.2 | Echocardiogram

Transthoracic echocardiogram (TTE) is often felt to be the main investigative tool for accessing cardiac diseases, in part due to its simplicity and accessibility. It is non-invasive and uses ultrasonic waves to provide information on the myocardium size and structure, blood flow, valvular function including any stenosis or regurgitation and any evidence of tissue damage. It is also able to give a relatively accurate estimate of cardiac output and ejection fraction. In clinical use, it also provides useful evidence of wall motion abnormality which can be related to myocardial ischaemia or previous infarcts. Due to the orientation of the heart and anatomical shape of the right ventricle, the imaging of the right heart proves to be a greater challenge. Due to the specific and complex geometry of the RV, many calculations and measurements of the RV can be difficult to obtain accurately and may represent an under and overestimation of RV pressure and function.

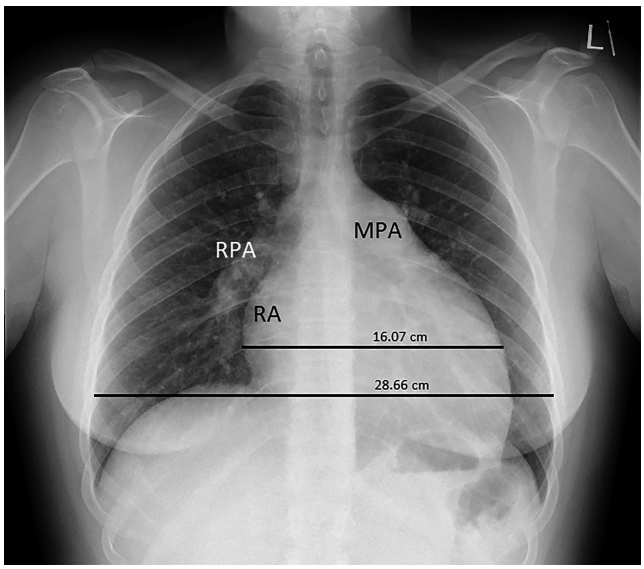

FIGURE 1 Chest x-ray demonstrating an enlarged main pulmonary artery (MPA) and a prominent right pulmonary artery (RPA). The cardiothoracic ratio is >0.5 reflecting cardiomegaly. The right heart is dilated as evidenced by the prominent right atrium (RA)

TTE is commonly performed using three windows—parasternal, apical and subcostal views, via different echo modalities. There are a number of different echo modalities including 2D, 3D and 4D echocardiography, but detailed examination of these is beyond the scope of this review. Continuous wave Doppler assesses dynamic blood flow and is used to estimate pulmonary artery systolic and diastolic pressure. A summary table of possible echocardiogram findings of the right ventricle in patients with pulmonary hypertension is shown below (Table 1) . The presence of these changes is dependent on how significant the severity of pulmonary hypertension is.

An estimated right ventricular systolic pressure can be calculated, which gives an indication as to whether a patient has pulmonary hypertension during screening, and if so, estimates severity. To provide an estimation of pulmonary artery pressure, the maximum velocity of blood through a regurgitant tricuspid valve (TRvmax) is measured using continuous wave Doppler, from which the peak tricuspid valve pressure gradient (TRPG) can be calculated using the simplified Bernoulli equation; $TRPG = 4 \times (TRVmax)^2$. An estimation of right atrial pressure (RAP) is added to the TRPG to estimate the right ventricular systolic pressure (RVSP). $RVSP = RAP + TRPG\ (4(TRVmax)^2)$ (Frost et al., 2019). Alternative aetiologies that may lead to increased right ventricular pressures include valvular abnormalities, left-sided heart disease and right ventricular outflow tract obstruction, which may be detected on TTE .

In the absence of right ventricular outflow obstruction, RVSP is equal to the systolic pulmonary artery pressure (SPAP). A TRPG ≤31 mm Hg suggests a low probability of PH, whilst ≥46 mm Hg gives a high probability. Other predictors of pulmonary hypertension can be obtained from TTE, including the pulmonary valve acceleration time (reduced in PH), the RV:LV basal diameter ratio (increased) and the pulmonary artery diameter (increased) (Frost et al., 2019).

RV size is measured at end-diastole and the mid-RV diameter is measured at the level of the LV papillary muscles; a diameter of >35 mm is considered abnormal. TTE should provide data on the estimated severity of PH through determining RV dysfunction. The longitudinal RV function is assessed by calculating a parameter known as TAPSE. This represents the deviation of the tricuspid annulus towards to RV apex as the tricuspid annular plane systolic excursion (TAPSE); a shortened TAPSE (<1.8 cm) suggests RV remodelling and systolic dysfunction and is associated with a poorer prognosis with patients (Forfia et al., 2006). Pericardial effusions rarely cause haemodynamic compromise in PH; however, any evidence of pericardial effusions is associated with increased mortality and reflects disease severity (Fenstad et al., 2013). The right atrial area is correlated to the extent of right atrial pressure and consequently a RA

TABLE 1 Echocardiogram findings of the right ventricle in pulmonary hypertension

	Pulmonary hypertension
Parasternal view	• RV wall dilated and hypertrophy • Consequential reduction in LV size with septal bowing towards LV (D-shape) • Dilatation of the main pulmonary artery • Atrial septal defect • Structural valvular abnormalities • RVOT abnormalities
Apical 4-chamber view	• RV dilatation and hypertrophy • RV apex usually hypertrophic and akinetic • RV systolic and diastolic dysfunction • Reduced myocardial tissue velocities • Tricuspid regurgitation with estimated TR velocity • Decreased TAPSE
Subcostal view	• Best view for RV inferior wall thickness and determines degree of dysfunction

area > 27 cm^2 is associated with a higher mortality (Bustamante-Labarta et al., 2002).

As discussed, as the right-sided pressure increases, the shape of the RV changes to a rounded structure, which compresses the LV in diastole. This can be visualised on TTE as causing a D-shaped LV. The interventricular septum will shift in diastole and the left ventricular eccentricity index (LVEI) can measure this effect by taking the ratio of two diameters of the LV measured at fixed points. This reflects external compression from a pressure- and volume-overloaded RV onto the LV with a LVEI >1.7 denoting a higher risk of mortality (Ghio et al., 2010). As discussed below, a comprehensive echocardiogram assessment involves imaging the venous system, including the collapsibility of the inferior vena cava and hepatic veins, in order to assess for evidence of right heart failure.

4.3 | Computed tomography (CT)

Computed tomography refers to a specific type of non-invasive imaging. It uses a rotating X-ray tube and a row of detectors to measure x-ray attenuations by different tissues inside the body. This allows a cross-sectional image to be produced from x-rays taken at multiple different angles.

CT imaging of the thorax provides excellent structural information on cardiopulmonary vasculature and lung parenchyma which can help determine aetiology of pulmonary hypertension. It is fast, easily accessible and has a quick scan time. However, CT scans are not useful in determining the right ventricular function as it lacks haemodynamic information. The use of CT is also limited due to ionising radiation, making it a less attractive option for patients who require serial imaging.

FIGURE 2 Transverse slice of a thoracic computed tomography image. The main pulmonary (MPA) is dilated, measuring 37.8 mm (normal is <27 mm in females, and < 29 mm in males) and is significantly larger than the 21.4 mm ascending aorta (Ao), with a ratio of 1.7 (>1.0 is abnormal). The right pulmonary artery (RPA) and left pulmonary artery (LPA) are dilated. DAo; descending thoracic aorta, SVC; superior vena cava

In pulmonary hypertension, the CT imaging of choice is the CT pulmonary angiogram (CTPA), which is contrast mediated and delineates the pulmonary trunk and associated vessels. This provides detailed information on acute or chronic pulmonary embolic disease and therefore allows radiographic assessment of chronic thromboembolic pulmonary hypertension (Kim et al., 2019). High-resolution CT thorax (HRCT) is also routinely required; this is non-contrast mediated and provides detailed imaging of the lung parenchyma.

There are key structures that are of importance when assessing the pulmonary vasculature and right ventricle by using CT.

4.3.1 | A—Pulmonary artery (PA)

A pulmonary artery diameter size of >29 mm in males and > 27 mm in females represents an abnormal enlargement and is usually due to dilatation of the main pulmonary artery trunk. An additional measurement is to compare the size of the pulmonary artery to the size of the aorta at the level of pulmonary artery bifurcation, with a ratio of >0.9 suggestive of PH (Truong et al., 2012) (Figure 2).

4.3.2 | B—Pulmonary vessels

Contrast CT is useful in delineating the pulmonary vessels. This is particularly helpful in assessing for chronic thromboembolic disease with typical findings including eccentric thrombi, intraluminal filling defects, intraluminal fibrous webbings or total occlusions. The presence of bronchial artery hypertrophy and bronchial artery collaterals suggest chronic occlusion since vascular remodelling has occurred to maintain vascular supply. Pulmonary arteriovenous malformation and pulmonary vein stenosis can also be detected on CT images.

4.3.3 | C—Right ventricle

Specific CT findings include thickening of the RV wall, dilatation of the RV cavity and bowing of the interventricular septum. Although not as specific or sensitive as echocardiography, CT can provide useful assessment of RV shape and size (Figure 3).

4.3.4 | D—Lung parenchyma

Non-contrast CT images are useful in this context in assessing for the presence of any lung disease that may be contributing to pulmonary hypertension—including interstitial pulmonary fibrosis, chronic obstructive pulmonary disease (COPD) and emphysema.

Other findings can include mediastinal and hilar lymphadenopathy, which is common in sarcoidosis.

The presence of thickened interlobular septa and bilateral effusions suggests the possibility of pulmonary veno-occlusive disease, especially when found in combination with centrilobular ground-glass opacities and lymph node enlargement.

4.3.5 | E—Pericardium

The finding of a pericardial effusion is non-specific, but the presence of it predicts a worse prognosis for PH patients.

4.3.6 | F—Other

CT thorax is also useful in assessing for cardiovascular causes of PH such as intracardiac defects with a resulting systemic to pulmonary shunt. Group 2 PH result from left heart disease and may be discernible on CT images by means of LV dilatation, left atrium dilatation and aortic or mitral valve pathology. Pleural effusions on CT images are non-specific and are associated with multiple conditions.

There are several types of CT acquisition—the choice of which is dependent on the clinical picture.

- *Single energy CT (SECT)*
  Conventional CT uses a single x-ray bean, received by a single detector. This is fast and relatively accessible and provides excellent cardiopulmonary structural information. Both contrast and non-contrast images can be acquired. As above, CTPA and HRCT are used in conjunction to provide a comprehensive evaluation of the cardiopulmonary structures.
- *Dual energy CT (DECT)*
  DECT combines traditional tomographic images with the addition of iodine mapping which is a surrogate of pulmonary perfusion, and as such perfusion defects can be analysed, allowing for both physiology and anatomy of the lungs to be studied simultaneously.
- *Single-photon emission computed tomography (SPECT)*
  SPECT is a nuclear medicine imaging technique, using a gamma-emitting radioisotope given intravenously which monitors the biological activity of the imaged organ.
  This is not routinely used in the assessment of PH patients and is more often used in myocardium stress testing, to aid in the diagnosis of ischaemic heart disease.

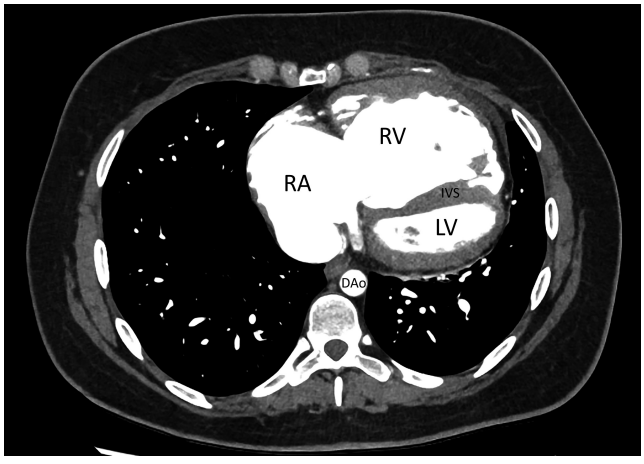

FIGURE 3 Transverse slice of a thoracic computed tomography image. The right atrium (RA) and right ventricle (RV) are grossly dilated and significantly larger than the left ventricle (LV) which is compressed. There is a displacement of the interventricular septum (IVS). Ao; descending thoracic aorta

4.4 | Cardiac magnetic resonance imaging (CMRI)

CMRI remains the gold standard non-invasive investigation in the diagnosis of PH, as it provides both anatomical and functional information of the right ventricle and pulmonary flow. It is the best non-invasive assessment of RV and LV stroke volume and cardiac output and is not limited by difficult acoustic windows. Whilst providing excellent functional and anatomical detail, it does not allow an estimation of pressure. CMRI is not operator dependent and is easily reproducible and, in comparison to the above imaging modalities, is far more comprehensive and superior in quality.

As it is non-invasive, highly specific and does not require ionising radiation, it is used for serial follow-ups to assess deterioration or response to therapy. However, there are limitations associated with this technique. The main limitations in clinical practice are the lack of trained expertise in data interpretation, high cost as well as patient claustrophobia. In comparison to CT, image acquisition for CMRI is timely and it can take up to an hour to obtain relevant imaging, limiting the number of scans performed during working hours. In addition, patients may need to breath-hold and in patients with significant cardiopulmonary disease, this can be difficult. CMRI software packages vary across different health boards, and depending on the manufacturer, this may result in variability and inconsistency in RV analysis. However, as technology advances, this is improving, and irregularities can be circumvented by using vendor-independent software.

CINE CMRI is a specific CMRI technique that displays the cardiac cycle in dynamic motion. This allows for the quantification of

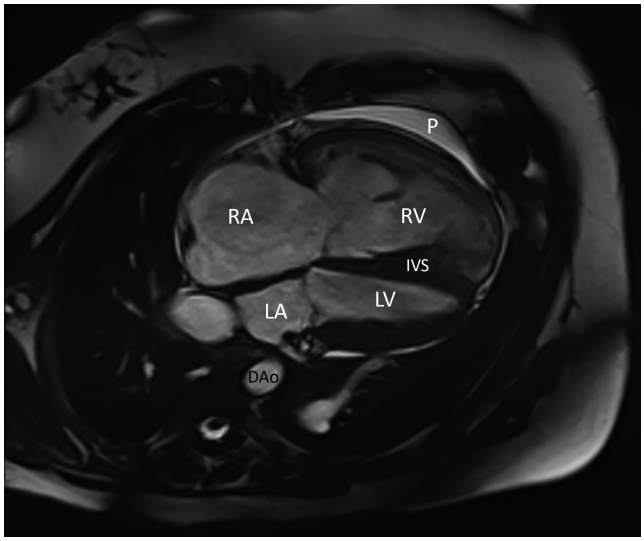

FIGURE 4 4-chamber view on cardiac MRI in a patient with pulmonary hypertension. The image demonstrates an enlarged right ventricle (RV) and right atrium (RA), a compressed left ventricle (LV) and left atrium (LA) with the displacement of the interventricular septum (IVS). The enhancing anterior rim reflects a small pericardial effusion (P). This would be in keeping with severe disease. Ao; descending thoracic aorta

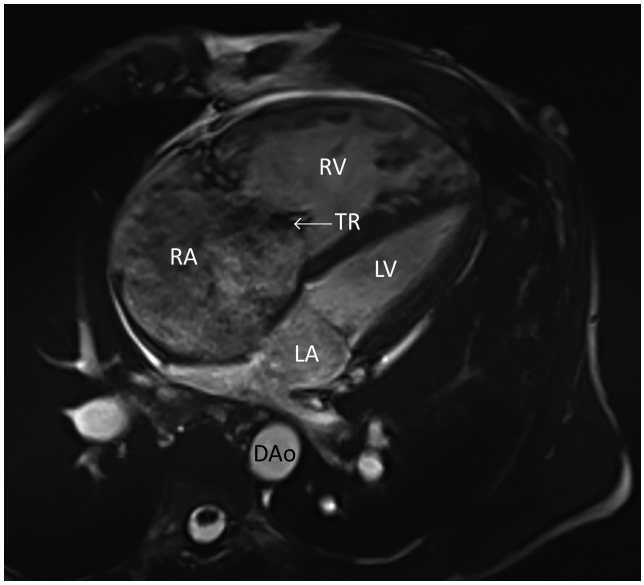

FIGURE 5 4-chamber view on cardiac MRI in a patient with pulmonary hypertension. This demonstrates a grossly dilated right atrium (RA) with an enlarged right ventricle (RV) and resulting compression of the left ventricle (LV). This view was taken in diastole, showing evidence of severe tricuspid regurgitation (TR) from the RV into the RA. Ao; descending thoracic aorta, LA; left atrium

ventricular mass, volumes and wall motion, which, in turn, translates to cardiac function.

The following are physiological CMRI variables of note in PH patients.

4.4.1 | A—Right ventri cle

Hypertrophy

RV hypertrophy is related to increased pressures of PH causing an increased afterload. It is defined as a RV wall thickness of >4 mm.

Dilatation

Dilatation of the RV is a consequence of RV failure as described above. It is defined as a RV:LV diameter ratio of >1 in axial images (Figure 4).

RV stroke volume

RV stroke volume refers to the amount of blood ejected from the RV during a single myocardial contraction. It is calculated by subtracting the total RV end-diastolic volume from the total RV end-systolic volume. *RV cardiac output* is subsequently calculated by multiplying stroke volume by heart rate, which, in turn, is an independent predictor of prognosis. Stroke volume, therefore, is an important determinant of cardiac function.

RV ejection fraction (RVEF)

RV dysfunction is defined as an RVEF of <45%. Traditionally pulmonary vascular resistance (PVR) is a measure of 'stiffness' of the pulmonary vasculature, and measurement of this can only be obtained after invasive measurement at right heart catheterisation; yet, RVEF at baseline has been shown to be more robust predictor of mortality than PVR (van de Veerdonk et al., 2011).

Ventricular mass ratio

Measurements of right ventricular mass/left ventricular mass ratio are a means of estimating mean pulmonary arterial pressure non-invasively. A ratio of >0.6 has a relatively high sensitivity and specificity for the diagnosis of PH (Saba et al., 2002).

4.4.2 | B—Left heart

The presence of left atrial dilatation, aortic and mitral valve pathology or left ventricular dysfunction may point to PH secondary to left-sided heart failure. This will not be covered in this paper. Compression of the left heart, which may lead to functional impairment, is quantifiable on CMRI and is an indicator of more severe disease (Figures 4 and 5).

4.4.3 | C—Interventricular septum

As mentioned, the IVS is normally rightward convex and in PH. In advanced PH, this septum eventually bows towards the left ventricle secondary to pressure overload. The RV becomes concentric subsequently, resulting in a reduced RVEF (Figure 4).

4.4.4 | D—Intracardiac shunts

Intracardiac shunts result in abnormal connections between the pulmonary and systemic circulation. Shunts are quantified by measuring the ratio of pulmonary blood flow (Qp) to systemic blood flow (Qs). In health, this ratio is 1 and so any increase would represent a significant shunt. Figure 6 represents an atrial septal defect (ASD), a form of congenital heart disease that can lead to PH (Simonneau et al., 2019).

4.4.5 | E—Pericardial effusion

As above, the presence of a pericardial effusion is a poor prognostic indicator (Figure 4) (Fenstad et al., 2013).

4.4.6 | F—Pulmonary artery

Measurement of pulmonary artery haemodynamics has been shown to correlate well with mean pulmonary artery pressure and pulmonary vascular resistance, both of which are raised in PH patients.

Pulmonary artery pulse-wave velocity (PWV)

PH leads to PA remodelling and can lead to increased transit time of a 'wave' propagating through an artery due to increased pressure.

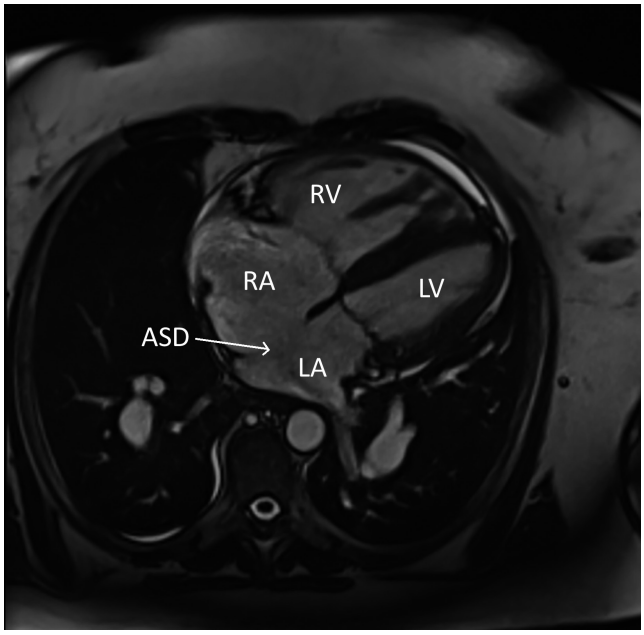

FIGURE 6 4-chamber view on cardiac MRI in a patient with congenital heart disease associated with pulmonary hypertension. This demonstrates an atrial septal defect (ASD) abnormal between the right atrium (RA) and left atrium (LA). RV; right ventricle, LV; left ventricle

This is a non-invasive measurement of pulmonary artery stiffness and is increased in PH patients (Forouzan et al., 2015).

Pulmonary artery relative area change (RAC)

Pulmonary artery RAC is another measurement of pulmonary artery stiffness and is defined as (maximal pulmonary artery area-minimum pulmonary artery area)/minimum pulmonary artery area. It is non-invasive and has been shown to predict mortality in patients with PAH (Gan et al., 2007).

There are now emerging modalities which use MRI as the basis of imaging but which give additional functional imaging.

- *CMR exercise stress*
  Stroke volume decreases during exercise as PH progresses. Exercise stress during CMRI, therefore, is useful in prognostication.
- *Others*
  Other features seen on CMRI that can help determine aetiology of PH are congenital cardiac disease, cardiomyopathies and aberrant pulmonary veins.
- *4D CMRI*
  In recent months, 4D CMRI is gaining traction in the screening of PH. In addition to the above, it is able to analyse pulmonary circulation and myocardial tissue in real time. This will likely be the preferred method of imaging in due course.
- *Late gadolinium enhancement*
  Gadolinium is a water-based contrast that is preferentially retained in fibrosed or infarcted tissue. This is often used to delineate other pathologies such as oedema, fatty infiltration or cardiac sarcoid involvement. Late gadolinium enhancement is often seen at the RV insertion point (RVIP) and is an indicator of more severe RV changes (Freed et al., 2012).

4.5 | Abdominal Ultrasonography (AUSS)

Medical ultrasonography utilises soundwaves, with frequencies higher than the range of human hearing. Ultrasonic images are created when pulses of ultrasound are reflected off different tissues, creating an acoustic impedance. Depending on the clinical need, different images can be obtained, including blood flow, stiffness of tissue and anatomy of specific organs. It is portable and relatively inexpensive and does not require ionising radiation. However, it is operator dependant, and imaging quality is subject to a patient's constitution and cooperation.

In patients with right ventricular failure, inferior vena cava and hepatic vein dilatation and backflow can arise from tricuspid regurgitation or impaired RV diastolic filling. Dilatation of these vessels can be visualised on an abdominal ultrasound, and a collapsibility index can be measured. This is useful in monitoring the effects of pulmonary hypertension therapy and can be used to identify systemic venous congestion in right heart failure (Pellicori et al., 2021). Furthermore, detection of a cirrhotic liver may give answers to the aetiology of the right heart failure and pulmonary hypertension.

In clinical practice, AUSS is seldom used for the evaluation of right heart failure, given it provides limited information on pulmonary vasculature or the myocardium in comparison to the above modalities.

In assessing the right ventricle structure and function, no imaging modality can be used in isolation. As discussed above, each format has advantages and drawbacks; yet, each helps to provide essential data in the structure and function of this complex organ. In clinical practice, these investigations are used in tandem for a holistic approach to managing a patient with pulmonary hypertension.

5 | CONCLUSION

Historically, the right ventricle has been seen as less important than the left ventricle; a view which is changing. The right ventricle is a complex structure with individualised anatomy which leads to distinct and unique functional capacity. The imaging of this structure has improved recently and novel techniques allow both structure and function to be analysed. This has led to enhanced understanding of the healthy right ventricle and subsequently a better appreciation of its role in disease. In certain key diseases, such as pulmonary arterial hypertension, impairment of RV function predicts outcomes for those patients. An understanding of RV anatomy, and how derangement in structure and function can be clinically assessed with imaging, is vital in diagnosing and monitoring this disease.

ACKNOWLEDGEMENTS

The authors would like to thank the patients who provided consent and allowed us to include the images within this article.

CONFLICT OF INTEREST

None of the authors have a conflict of interest in relation to this submission.

AUTHOR CONTRIBUTIONS

Dr Stubbs, Dr MacLellan and Dr Lua each provided one of the three sections and provided equal input into the manuscript. Dr Helen Dormand provided expertise in the selection and curation of suitable images. Dr Church provided oversight and editorial expertise.

CONSENT

Patient images have been included within this manuscript. We can confirm that all patients have provided written consent in agreement for their anonymised images to be included, shared and disseminated.

DATA AVAILABILITY STATEMENT

N/A

ORCID

Harrison Stubbs https://orcid.org/0000-0003-1786-342X
Alexander MacLellan https://orcid.org/0000-0003-3436-9925
Colin Church https://orcid.org/0000-0002-4446-0100

REFERENCES

Almedia, M.C., Stephenson, R.S., Anderson, R.H., Benvenuti, L.A., Loukas, M. & Aiello, V. (2020) Human subpulmonary infundibulum has an endocardial network of specialized conducting cardiomyocytes. *Heart Rhythm*, 17(1), 123–130.

Anderson, R.H., Webb, S., Brown, N.A., Lamers, W. & Moorman, A. (2003) Development of the heart: (2) septation of the atriums and ventricles. *Heart (British Cardiac Society)*., 89(8), 949–958.

Baggen, V.J., Leiner, T., Post, M.C., van Dijk, A.P., Roos-Hesselink, J.W., Boersma, E. et al. (2016) Cardiac magnetic resonance findings predicting mortality in patients with pulmonary arterial hypertension: a systematic review and meta-analysis. *European Radiology*, 26(11), 3771–3780.

Bidviene, J., Muraru, D., Maffessanti, F., Ereminiene, E., Kovács, A., Lakatos, B. et al. (2021) Regional shape, global function and mechanics in right ventricular volume and pressure overload conditions: a three-dimensional echocardiography study. *The International Journal of Cardiovascular Imaging*, 37(4), 1289–1299.

Bustamante-Labarta, M., Perrone, S., Leon De La Fuenta, R., Stutzbach, P., Pere De La Hoz, R., Torino, A. et al. (2002) Right atrial size and tricuspid regurgitation severity predict mortality or transplantation in primary pulmonary hypertension. *Journal of the American Society of Echocardiography: Official Publication of the American Society of Echocardiography*, 15(10 Pt 2), 1160–1164.

Courand, P.Y., Jomir, G.P., Khouatra, C., Scheiber, C., Turquier, S., Glerant, J.C. et al. (2015) Prognostic value of right ventricular ejection fraction in pulmonary arterial hypertension. *The European Respiratory Journal*., 45(1), 139–149.

Dahou, A., Levin, D., Reisman, M. & Hahn, R. (2019) Anatomy and physiology of the tricuspid valve. *JACC Cardiovascular Imaging*., 12(3), 458–468.

Daniel, G. & Walton, L.G. (1975) Congenital malformations of the heart. In: *Illustrated*, 1st edition. New York: Grune & Stratton.

Dong, Y., Sun, J., Yang, D., He, J., Cheng, W., Wan, K. et al. (2018) Right ventricular septomarginal trabeculation hypertrophy is associated with disease severity in patients with pulmonary arterial hypertension. *The International Journal of Cardiovascular Imaging*, 34(9), 1439–1449.

Fenstad, E.R., Le, R.J., Sinak, L.J., Maradit-Kremers, H., Ammash, N.M., Ayalew, A.M. et al. (2013) Pericardial effusions in pulmonary arterial hypertension: characteristics, prognosis, and role of drainage. *Chest*, 144(5), 1530–1538.

Foale, R., Nihoyannopoulos, P., McKenna, W., Kleinebenne, A., Nadazdin, A., Rowland, E. et al. (1986) Echocardiographic measurement of the normal adult right ventricle. *British Heart Journal*, 56(1), 33–44.

Forfia, P.R., Fisher, M.R., Mathai, S.C., Housten-Harris, T., Hemnes, A.R., Borlaug, B.A. et al. (2006) Tricuspid annular displacement predicts survival in pulmonary hypertension. *American Journal of Respiratory and Critical Care Medicine*, 174(9), 1034–1041.

Forouzan, O., Warczytowa, J., Wieben, O., Francois, C.J. & Chesler, N.C. (2015) Non-invasive measurement using cardiovascular magnetic resonance of changes in pulmonary artery stiffness with exercise. *Journal of Cardiovascular Magnetic Resonance: Official Journal of the Society for Cardiovascular Magnetic Resonance*., 17(109), 109.

Freed, B.H., Gomberg-Maitland, M., Chandra, S., Mor-Avi, V., Rich, S., Archer, S.L. et al. (2012) Late gadolinium enhancement cardiovascular magnetic resonance predicts clinical worsening in patients with pulmonary hypertension. *Journal of Cardiovascular Magnetic Resonance: Official Journal of the Society for Cardiovascular Magnetic Resonance*, 14(1).

Frost, A., Badesch, D., Gibbs, J.S.R., Gopalan, D., Khanna, D., Manes, A. et al. (2019) Diagnosis of pulmonary hypertension. *European Respiratory Journal*, 53(1).

Gan, C.T., Lankhaar, J., Westerhof, N., Marcus, J.T., Becker, A., Twisk, J.W.R. et al. (2007) Noninvasively assessed pulmonary artery stiffness predicts mortality in pulmonary arterial hypertension. *Chest*, 132(6), 1906–1912.

Ghio, S., Klersy, C., Magrini, G., D'Armini, A.M., Scelsi, L., Raineri, C. et al. (2010) Prognostic relevance of the echocardiographic assessment of right ventricular function in patients with idiopathic pulmonary arterial hypertension. *International Journal of Cardiology.*, 140(3), 272–278.

Gomez-Arroyo, J., Santos-Martinez, L.E., Aranda, A., Pulido, T., Beltran, M., Muñoz-Castellanos, L. et al. (2014) Differences in right ventricular remodeling secondary to pressure overload in patients with pulmonary hypertension. *American Journal of Respiratory and Critical Care Medicine*, 189(5), 603–606.

Strandring, S. (Ed.). (2020) Heart. *Gray's anatomy - the anatomical basis of clinical practice*, 42nd edition. Amsterdam: Elsevier, pp. 1068–1096.

Hayes, D.L. & Furman, S. (2004) Cardiac pacing: how it started, where we are, where we are going. *Heart Rhythm*, 1(5 Suppl), 693–704.

Ho, S.Y. & Nihoyannopoulos, P. (2006) Anatomy, echocardiography, and normal right ventricular dimensions. *Heart (British Cardiac Society)*, 92(Suppl 1), i2–i13.

Kim, N.H., Delcroix, M., Jais, X., Madani, M.M., Matsubara, H., Mayer, E. et al. (2019) Chronic thromboembolic pulmonary hypertension. *European Respiratory Journal*, 53(1).

Kind, T., Mauritz, G.J., Marcus, J.T., van de Veerdonk, M., Westerhof, N. & Vonk-Noordegraaf, A. (2010) Right ventricular ejection fraction is better reflected by transverse rather than longitudinal wall motion in pulmonary hypertension. *Journal of Cardiovascular Magnetic Resonance*, 12, 35.

Kovacs, A., Lakatos, B., Tokodi, M. & Merkely, B. (2019) Right ventricular mechanical pattern in health and disease: beyond longitudinal shortening. *Heart Failure Reviews*, 24(4), 511–520.

Kovacs, G., Berghold, A., Scheidl, S. & Olschewski, H. (2009) Pulmonary arterial pressure during rest and exercise in healthy subjects: a systematic review. *The European Respiratory Journal*, 34(4), 888–894.

Kukulski, T., Hubbert, L., Arnold, M., Wranne, B., Hatle, L. & Sutherlands, G.R. (2000) Normal regional right ventricular function and its change with age: a doppler myocardial imaging study. *Journal of the American Society of Echocardiography: Official Publication of the American society of Echocardiography*, 13(3), 194–204.

Lewis, R.A., Durrington, C., Condliffe, R. & Kiely, D.G. (2020) BNP/NT-proBNP in pulmonary arterial hypertension: time for point-of-care testing? *European Respiratory Review*, 29(156).

Loukas, M., Klaassen, Z., Tubbs, R.S., Derderian, T., Paling, D., Chow, D. et al. (2010) Anatomical observations of the moderator band. *Clinical Anatomy*, 23(4), 443–450.

Lyon, R.C., Zanella, F., Omens, J.H. & Sheikh, F. (2015) Mechanotransduction in cardiac hypertrophy and failure. *Circulation Research*, 116(8), 1462–1476.

Mahadevan, V. (2015) Anatomy of the heart. *Surgery*, 33(2), 47–51.

Moorman, A., Webb, S., Brown, N.A., Lamers, W. & Anderson, R.H. (2003) Development of the heart: (1) formation of the cardiac chambers and arterial trunks. *Heart (British Cardiac Society)*, 89(7), 806–814.

Morton, S. & Brodsky, D. (2016) Fetal physiology and the transition to extrauterine life. *Clinics in Perinatology*, 43(3), 395–407.

Naeije, R. & Badagliacca, R. (2017) The overloaded right heart and ventricular interdependence. *Cardiovascular Research*, 113(12), 1474–1485.

Nielsen, E., Smerup, M., Agger, P., Frandsen, J., Ringgard, S., Pedersen, M. et al. (2009) Normal right ventricular three-dimensional architecture, as assessed with diffusion tensor magnetic resonance imaging, is preserved during experimentally induced right ventricular hypertrophy. *The Anatomical Record*, 292(5), 640–651.

Noordegraaf, A.V., Chin, K.M., Haddad, F., Hassoun, P.M., Hemnes, A.R., Hopkins, S.R. et al. (2019) Pathophysiology of the right ventricle and of the pulmonary circulation in pulmonary hypertension: an update. *European Respiratory Journal*, 53(1), 1801900.

Pellicori, P., Platz, E., Dauw, J., Maaten, J.M.T., Martens, P., Pivetta, E. et al. (2021) Ultrasound imaging of congestion in heart failure: examinations beyond the heart. *European Journal of Heart Failure*, 23(5), 703–712.

Rao, S.D., Menachem, J.N., Birati, E.Y. & Mazurek, J.A. (2019) Pulmonary hypertension in advanced heart failure: assessment and management of the Failing RV and LV. *Current Heart Failure Reports*, 16(5), 119–129.

Rigolin, V.H., Robiolio, P.A., Wilson, J.S., Harrison, J.K. & Bashore, T.M. (1995) The forgotten chamber: the importance of the right ventricle. *Catheterization and Cardiovascular Diagnosis*, 35(1), 18–28.

Robert, A., Diane, S., Anthony, H., Andrew, C. & Carl, B. (2013) *Wilcox's surgical anatomy of the heart*, 4th edition. Cambridge: Cambridge University Press.

Rodrigues, S.L., Pimentel, E.B. & Geraldo, M.J. (2007) Cardiac ventricular weights recorded at the autopsy of healthy subjects who died of external causes. *Arquivos Brasileiros De Cardiologia.*, 89(5), 279–284.

Rubin, L.J. & Physicians ACoC. (2004) Diagnosis and management of pulmonary arterial hypertension: ACCP evidence-based clinical practice guidelines. *Chest*, 126(1 Suppl), 7S–10S.

Ryan, J.J. & Archer, S.L. (2014) The right ventricle in pulmonary arterial hypertension: disorders of metabolism, angiogenesis and adrenergic signaling in right ventricular failure. *Circulation Research*, 115(1), 176–188.

Saba, T.S., Foster, J., Cockburn, M., Cowan, M. & Peacock, A.J. (2002) Ventricular mass index using magnetic resonance imaging accurately estimates pulmonary artery pressure. *The European Respiratory Journal*, 20(6), 1519–1524.

Sanz, J., Sánchez-Quintana, D., Bossone, E., Bogaard, H.J. & Naeije, R. (2019) Anatomy, function, and dysfunction of the right ventricle: JACC state-of-the-art review. *Journal of the American College of Cardiology*, 73(12), 1463–1482.

Simonneau, G., Montani, D., Celermajer, D.S., Denton, C.P., Gatzoulis, M.A., Krowka, M. et al. (2019) Haemodynamic definitions and updated clinical classification of pulmonary hypertension. *The European Respiratory Journal*, 53(1).

Tan, C.M.J. & Lewandowski, A.J. (2020) The transitional heart: from early embryonic and fetal development to neonatal life. *Fetal Diagnosis and Therapy*, 47(5), 373–386.

Tan, R.T., Juzo, R., Goodman, L.R., Siegel, R., Haasler, G.B. & Presberg, K.W. (1998) Utility of CT scan evaluation for predicting pulmonary hypertension in patients with parenchymal lung disease. Medical College of Wisconsin lung transplant group. *Chest*, 113(5), 1250–1256.

Tezuka, F., Hort, W., Lange, P.E. & Nürnberg, J.H. (1990) Muscle fiber orientation in the development and regression of right ventricular hypertrophy in pigs. *Acta Pathologica Japonica*, 40(6), 402–407.

Tomanek, R. & Angelini, P. (2019) Embryology of coronary arteries and anatomy/pathophysiology of coronary anomalies. A comprehensive update. *International Journal of Cardiology.*, 281, 28–34.

Truong, Q.A., Massaro, J.M., Rogers, I.S., Mahabadi, A.A., Kriegel, M.F., Fox, C.S. et al. (2012) Reference values for normal pulmonary artery dimensions by noncontrast cardiac computed tomography: the Framingham heart study. *Circulation Cardiovascular Imaging*, 5(1), 147–154.

van de Veerdonk, M.C., Kind, T., Marcus, J.T., Mauritz, G.J., Heymans, M.W., Bohaard, H.J. et al. (2011) Progressive right ventricular dysfunction in patients with pulmonary arterial hypertension responding to therapy. *Journal of the American College of Cardiology*, 58(24), 2511–2519.

van Wolferen, S.A., Marcus, J.T., Westerhof, N., Spreeuwenberg, M.D., Marques, K.M., Bronzwaer, J.G. et al. (2008) Right coronary artery flow impairment in patients with pulmonary hypertension. *European Heart Journal*, 29(1), 120–127.

Voelkel, N.F., Quaife, R., Leinwand, L.A., Barst, R.J., McGoon, M.D., Meldrum, D.R. et al. (2006) Right ventricular function and failure: report of a National Heart, Lung, and Blood Institute working group on cellular and molecular mechanisms of right heart failure. *Circulation*, 114(17), 1883–1891.

Vonk-Noordegraaf, A., Haddad, F., Chin, K.M., Forfia, P.R., Kawut, S.M., Lumens, J. et al. (2013) Right heart adaptation to pulmonary arterial hypertension: physiology and pathobiology. *Journal of the American College of Cardiology*, 62(25 Suppl), D22–D33.

Zong, P., Tune, J.D. & Downey, H.F. (2005) Mechanisms of oxygen demand/supply balance in the right ventricle. *Experimental Biology and Medicine*, 230(8), 507–519.

How to cite this article: Stubbs, H., MacLellan, A., Lua, S., Dormand, H. & Church, C. (2023) The right ventricle under pressure: Anatomy and imaging in sickness and health. *Journal of Anatomy*, 242, 17–28. Available from: https://doi.org/10.1111/joa.13654